Tracking Fast Inverted Trajectories of the Underactuated Acrobot

Matthew D. Berkemeier and Ronald S. Fearing

***Abstract*— The control of underactuated robot manipulators provides a significant challenge to the robotics engineer. The Acrobot is a simple underactuated system consisting of a double pendulum with an actuator at only the second joint. Previous work has shown how linearization methods can achieve the tracking of slow inverted trajectories. In this paper we derive a surprising set of exact trajectories of the nonlinear equations of motion, which involve inverted periodic motions. The trajectories can be made arbitrarily fast by appropriate choice of the Acrobot mass and length parameters. Next, we present a nonlinear control law (which has appeared elsewhere) and show how it can be applied to the Acrobot to track these trajectories. In simulations we compare tracking results for our controller and one based on pseudolinearization. The pseudolinearizing controller produces significant error for a 1 Hz trajectory, while ours produces none. Finally, we present experimental results which demonstrate that the assumptions of the theory were not overly restrictive. In particular, peak-to-peak oscillations of joint 2 as large as 85° were obtained, despite real-world effects, such as joint friction, inexact parameter values, and noisy and delayed joint velocity data.**

***Index Terms*— Acrobot, double pendulum, nonlinear control, underactuated.**

I. Introduction

STRAIGHTFORWARD approaches exist for the stabilization and tracking control of fully-actuated, serial-link manipulators (e.g., PID, computed torque). However, the absence of just one actuator changes things considerably. For example, it is not possible to follow arbitrary paths in configuration space. As yet, there is no comprehensive theory for underactuated robot manipulators, i.e., manipulators having fewer actuators than degrees of freedom. However, this class of manipulators has received significant attention over the last few years. Frequently cited applications include saving weight and energy by using fewer actuators and gaining fault tolerance to actuator failure. The challenge of solving control problems associated with this class of systems will stimulate new results in robot control theory in the years to come.

One simplifying approach, which leads to specific algorithms for moving from one configuration to another, is to assume that the unactuated joints are equipped with simple brakes which can lock or unlock the joint. This was the basis for work by Arai *et al.* [1], [2] and more recently by Bergerman *et al.* [5], [6]. Jain and Rodriguez [13] developed generalized kinematics and dynamics concepts for underactuated manipulators including generalized Jacobian matrices and a computationally efficient approach to finding the equations of motion. Baillieul [3] considered the effect of rapid periodic forcing of actuated degrees of freedom in order to effect unactuated degrees of freedom. Seto and Baillieul [23] used Control Flow Diagrams to help classify underactuated systems. For a limited set of systems they were able to apply stabilizing and tracking control laws.

Some researchers have recognized that underactuated mechanical systems can be interpreted as systems with second order nonholonomic constraints [e.g., the first row of (1) can be interpreted as a second-order nonholonomic constraint]. Certainly, there has been much progress in recent years on systems with first order nonholonomic constraints [15], and thus a similar line of study may also provide results for underactuated robot manipulators. For pioneering work in this area, see the papers by Oriolo and Nakamura [18] and Reyhanoglu *et al.* [21].

The Acrobot (for acrobatic robot) is a simple example of an underactuated robot manipulator consisting of a double pendulum with an actuator at only the second joint (Fig. 1). It was originally envisioned as a rough model of a human gymnast on a high bar, where the unactuated first joint modeled the degree of freedom of a gymnast's hands on the bar (if there were little friction), and the actuated second joint modeled the gymnast's hip. The Acrobot was studied by Hauser and Murray [10]. The following basic results come from their paper.

1) The Jacobian linearization about any of the inverted equilibrium states, where there center of mass is directly above the first joint, is completely controllable.
2) The Acrobot is not exactly input-state linearizable (i.e., there does not exist a combination of static nonlinear feedback and nonlinear coordinate transformation to make the equations of motion linear).

They applied an approximate linearization approach, in which they derived a new nonlinear system which was similar to the Acrobot near the equilibrium manifold but which was exactly linearizable. Then, they used the associated feedback control to cause the Acrobot to follow trajectories which were close to the equilibrium manifold. In a more detailed presentation [17] their controller showed good performance for a 0.08 Hz inverted periodic trajectory. A somewhat similar approach was used by Bortoff and Spong [9]. They avoided

Manuscript received September 3, 1996; revised April 13, 1999. This paper was recommended for publication by Associate Editor R. Chatila and Editor A. Goldenberg upon evaluation of the reviewers' comments.

M. D. Berkemeier is with the Department of Electrical and Computer Engineering, Utah State University, Logan, UT 84322-4120 USA.

R. S. Fearing is with the Department of Electrical Engineering and Computer Science, University of California at Berkeley, Berkeley, CA 94720-1770 USA.

Publisher Item Identifier S 1042-296X(99)05401-4.

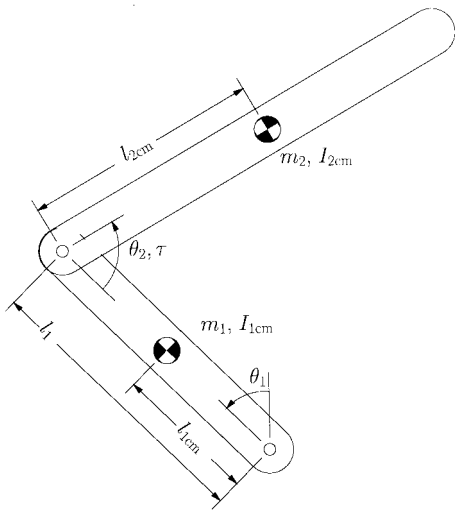

Fig. 1. Acrobot parameters.

computationally expensive calculations through use of spline approximations and implemented their controller on a physical Acrobot. In [8] Bortoff demonstrated good tracking for a 0.077 Hz trajectory but rather poor tracking for a 0.15 Hz trajectory in experiments. A slight variation on the Acrobot makes joint 1 actuated. Bedrossian [4] used yet another linearization approach on this system. Pannu *et al.* [19] derived a robust linear feedback control based on the linear approximation of the Acrobot at a single equilibrium. Experiments on a physical system verified the method. They planned to apply this to a bipedal walking robot.

In addition to inverted equilibrium stabilization, or the tracking of inverted trajectories, others have considered different goals for the Acrobot. Spong [24] considered the "swing-up" problem, i.e., going from hanging straight down to standing straight up. He exactly linearized dynamics of either the first or second joint as part of his approach. Lee and Smith [16] also looked at the swing-up problem but used fuzzy control methods instead. Saito *et al.* [22] were able to make a two-link robot swing from rung to rung on a ladder-like apparatus, mimicking monkey locomotion. Heuristic feedforward and feedback control methods were used. With one end of the two-link robot free and the other grasping a rung, the dynamics of the brachiating robot were the same as the Acrobot.

Our approach in this paper is most similar to the work of [4], [9], [10], [19], but there are significant differences as well: rather than relying on a linear approximation of the Acrobot near the set of equilibrium states, we have found a surprising set of exact trajectories of the nonlinear equations. This provides the potential for tracking fast inverted trajectories. Our experimental results in Section V demonstrate tracking of 0.63 Hz trajectories.

In Section II we describe the special set of periodic inverted motions for the Acrobot. Section III describes our control law and how it can be applied to the Acrobot to track the trajectories of Section II. In Section IV we present simulation results to compare our approach to pseudolinearization. Section V describes our experimental setup and results. Finally, we offer our conclusions in Section VI.

II. Acrobot Model

A. Equations of Motion

Fig. 1 shows the notation and conventions used for the Acrobot parameters and variables. The equations of motion are written in the standard form [26] below: $M(\theta)$ is symmetric and positive definite, and $C(\theta,\dot\theta)$ has been chosen such that $\dot M - 2C$ is skew symmetric. Note the 0 in the vector on the right side of (1), indicating the absence of an actuator at the first joint

$$M(\theta)\ddot\theta + C(\theta,\dot\theta)\dot\theta + N(\theta) = \begin{bmatrix}0\\ \tau\end{bmatrix} \tag{1}$$

$$M(\theta) = \begin{bmatrix} c_1 + c_2 - 2c_3\cos\theta_2 & c_2 - c_3\cos\theta_2 \\ c_2 - c_3\cos\theta_2 & c_2 \end{bmatrix}$$
$$C(\theta,\dot\theta) = \begin{bmatrix} c_3\dot\theta_2\sin\theta_2 & c_3(\dot\theta_1+\dot\theta_2)\sin\theta_2 \\ -c_3\dot\theta_1\sin\theta_2 & 0 \end{bmatrix}$$
$$N(\theta) = \begin{bmatrix} -c_4\sin\theta_1 + c_5\sin(\theta_1+\theta_2) \\ c_5\sin(\theta_1+\theta_2) \end{bmatrix}$$

where

$$c_1 = m_1 l_{1\mathrm{cm}}^2 + m_2 l_1^2 + I_{1\mathrm{cm}}, \quad c_2 = m_2 l_{2\mathrm{cm}}^2 + I_{2\mathrm{cm}},$$
$$c_3 = m_2 l_1 l_{2\mathrm{cm}},$$
$$c_4 = (m_1 l_{1\mathrm{cm}} + m_2 l_1)g, \quad c_5 = m_2 g l_{2\mathrm{cm}}$$

with

$$\theta = \begin{bmatrix}\theta_1\\ \theta_2\end{bmatrix}.$$

B. Some "Interesting" Trajectories

To derive the trajectories of interest, simply substitute

$$\theta_2 \equiv \phi - 2\theta_1 \tag{2}$$

into the first row of (1), where ϕ is an unspecified constant (We use "$\equiv$" to mean "equal for all time" or "identically equal to." This implies $\dot\theta_2 = -2\dot\theta_1$, $\ddot\theta_2 = -2\ddot\theta_1$, etc.) This gives

$$(c_1 - c_2)\ddot\theta_1 = c_4\sin\theta_1 + c_5\sin(\theta_1 - \phi). \tag{3}$$

Notice that a number of terms cancel when making the substitution to give the rather simple expression above. In fact, (3) is that of a single degree of freedom, unforced pendulum. To see this, note that the right side of (3) is

$$(c_4 + c_5\cos\phi)\sin\theta_1 - c_5\sin\phi\cos\theta_1$$

and also

$$a\sin\theta + b\cos\theta = \sqrt{a^2+b^2}\sin(\theta + \tan^{-1}(b/a)).$$

For well-chosen parameter values, the motion described by (2) and (3) corresponds to periodic *inverted* motion of the Acrobot. For example, choose $\phi = \pi$. Equation (3) then can be written

$$\ddot\theta_1 = \frac{c_4 - c_5}{c_1 - c_2}\sin\theta_1. \tag{4}$$

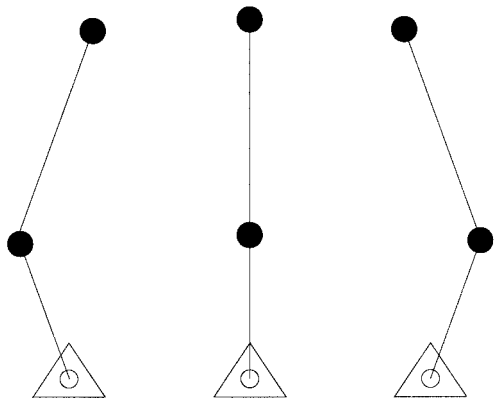

Fig. 2. Inverted oscillations of the acrobot. Imagine the Acrobot starts in the left configuration at rest. One quarter of a period later it will be in the middle configuration, and another quarter period will give the right picture. After a total of one period, it will be back in the left configuration.

We have frequently used the parameters

$$m_1 = m_2 = 7\,\text{kg}, \quad l_{1\text{cm}} = l_1 = 0.5\,\text{m}, \quad l_{2\text{cm}} = 0.75\,\text{m}$$
$$I_{1\text{cm}} = I_{2\text{cm}} = 0, \quad g = 10\,\text{m/s}^2$$

in our simulations, as they roughly correspond to a large Acrobot in the Berkeley EECS Robotics Lab (the zero inertias are due to point mass approximations). This makes the right side of (4) $-40\sin\theta_1$, and the minus sign means the Acrobot oscillates about its *inverted* (i.e., "straight up") configuration with the dynamics of a *noninverted*, single degree of freedom pendulum! Fig. 2 illustrates the Acrobot's motion corresponding to (4) and (2) (with $\phi = \pi$).

Conceptually, one can imagine using the single input, τ, to enforce the constraint in (2) (this will be made more precise a little later in the paper). Then θ_1 (the unactuated joint) will behave according to (3). This does not make an effective control approach, however, since (3) describes a set of trajectories, parameterized by oscillation amplitude, and disturbances and joint friction, for example, will cause shifting within this set.

To put this in some context, one can also look at the result of a simpler substitution, namely $\theta_2 \equiv \phi_2$, where ϕ_2 is an arbitrary constant. Again, one can think of this as a constraint to be enforced by the input τ. Making this substitution into the first row of (1) gives

$$(c_1 + c_2 - 2c_3\cos\phi_2)\ddot{\theta}_1 = c_4\sin\theta_1 - c_5\sin(\theta_1 + \phi_2).$$

The resulting dynamics are those of a single degree of freedom, unforced pendulum, as before. In this case, understanding the motion is much easier, however. The second joint is locked through use of the actuator at that joint, and the Acrobot swings freely at its unactuated first joint, just like a single degree of freedom pendulum. Of course, in this case, inverted oscillations do not occur.

One could also enforce the constraint $\theta_1 \equiv \phi_1$, and, in this case, the first joint would be locked and the second joint would have the dynamics of a pendulum. The constraint $\theta_2 \equiv \phi - 2\theta_1$ is the only constraint of the form $\theta_2 \equiv k_1\theta_1 + k_2$ $(k_1 \neq 0)$ which produces simple pendulum dynamics in the remaining degrees of freedom of the Acrobot. This can easily be seen by direct substitution of the constraint into the first row of (1). Conditions for inverted oscillations can be derived. For example, let $\phi = \pi$ and use the simplifying point mass approximation so that $I_{1\text{cm}} = I_{2\text{cm}} = 0$ and $l_{1\text{cm}} = l_1$, $l_{2\text{cm}} = l_2$. If the coefficient of $\sin\theta_1$ in (4) is negative, oscillations will occur about the straight up position, $(\theta_1, \theta_2) = (0, \pi)$. This corresponds to the following condition:

$$\frac{l_2}{l_1} < 1 + \frac{m_1}{m_2} < \left(\frac{l_2}{l_1}\right)^2. \tag{5}$$

Among other things, it is clear that we must have $l_2 > l_1$. At this time, we do not have a simple physical explanation for the inverted oscillations.

C. Significance of ϕ

The value of ϕ in (2) and (3) determines the configuration about which the oscillations occur. For example, for $\phi = \pi$ and parameters satisfying (5), the oscillations occur about $(\theta_1, \theta_2) = (0, \pi)$ (straight up). The configuration $(\theta_1, \theta_2) = (\pi, \pi)$ (i.e., hanging straight down) is also an equilibrium, but this corresponds to an unstable pendulum equilibrium for the same parameter values. More generally, the equilibrium configurations exist at values of θ_1 and θ_2 which are solutions to

$$0 = c_4\sin\theta_1 + c_5\sin(\theta_1 - \phi)$$
$$\theta_2 = \phi - 2\theta_1.$$

Physically, these correspond to configurations where the Acrobot's center of mass is located on a vertical line drawn through joint 1. This set of configurations, together with the specification of zero joint velocities, has been referred to as the Acrobot's *equilibrium manifold* by Hauser and Murray [10] since for every one of these configurations there exists a torque such that the Acrobot remains at the configuration if it starts there with no joint velocities. Thus, ϕ parameterizes the Acrobot's equilibrium manifold, and the oscillations given by (2) and (3) are about particular configurations on this manifold. Fig. 3 illustrates these ideas for the parameter values given earlier.

D. Interpretation in Terms of Zero Dynamics

Here we explain more precisely what was meant by using our input to enforce the constraint in (2). Consider the single input, single output nonlinear system

$$\dot{x} = f(x) + g(x)u, \qquad x \in \mathbb{R}^n$$
$$y = h(x) \tag{6}$$

where f and g are smooth n-dimensional vector fields, and h is a smooth, scalar-valued function. It is often possible to choose an input which makes $y \equiv 0$, assuming initial conditions are chosen correctly. To see this, we start by differentiating the

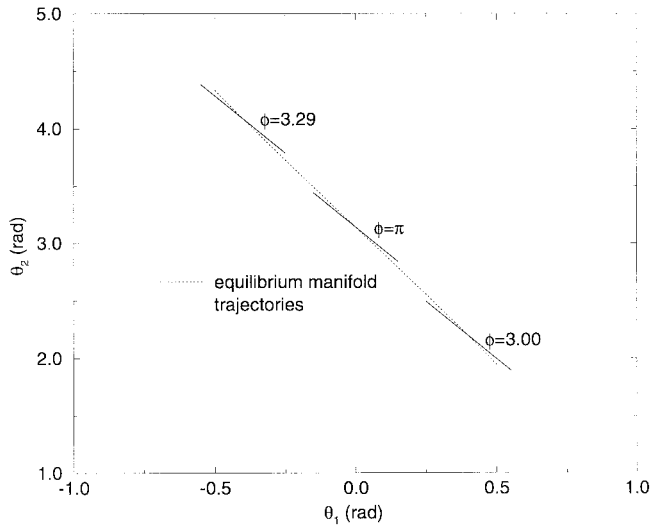

Fig. 3. Projection of the inverted equilibrium manifold and three trajectories onto the plane $\dot{\theta}_1 = \dot{\theta}_2 = 0$. Note that the equilibrium manifold would not extend out of this plane, but the trajectories would since they do not satisfy $\dot{\theta}_1 = \dot{\theta}_2 = 0$. Also, note that only a portion of the inverted equilibrium manifold is shown.

output equation

$$\begin{aligned}\dot{y} &= \frac{\partial h}{\partial x}(x)\dot{x} \\ &= \frac{\partial h}{\partial x}(x)(f(x)+g(x)u) \\ &= L_f h(x) + L_g h(x) u\end{aligned}$$

where the scalar-valued function $L_f h(x) = (\partial h/\partial x)(x) f(x)$ is the *Lie derivative of h along f* [11], and $L_g h(x)$ is defined analogously. If $L_g h(x^o) \neq 0$ for some x^o of interest, then the control system is said to have *relative degree* 1 at x^o, and we may choose

$$u = -\frac{L_f h}{L_g h}(x)$$

which will maintain $\dot{y} \equiv 0$ in some neighborhood of x^o. Furthermore, if we start with the initial condition $y = 0$, then it is clear that $y \equiv 0$ as desired. Now, if $L_g h(x) = 0$ for all x in a neighborhood of x^o, then we differentiate a second time

$$\begin{aligned}\ddot{y} &= \frac{\partial L_f h}{\partial x}(x)\dot{x} \\ &= L_f^2 h(x) + L_g L_f h(x) u\end{aligned}$$

where $L_f^2 h(x) = L_f(L_f h)(x)$. If $L_g L_f h(x^o) \neq 0$, then the system has relative degree 2 at x^o, and we choose

$$u = -\frac{L_f^2 h}{L_g L_f h}(x) \tag{7}$$

which makes $\ddot{y} \equiv 0$ in some neighborhood of x^o. If we start with initial conditions $y = \dot{y} = 0$, then $y \equiv 0$, as desired. This process can be continued in the obvious way, however, all we are interested in is the relative degree 2 case.

Now, write the Acrobot equations of motion in the form of (6)

$$\frac{d}{dt}\begin{bmatrix}\theta \\ \dot{\theta}\end{bmatrix} = \begin{bmatrix}\dot{\theta} \\ -M^{-1}(\theta)(C(\theta,\dot{\theta})\dot{\theta} + N(\theta))\end{bmatrix} + \begin{bmatrix}0 \\ M^{-1}(\theta)\begin{bmatrix}0 \\ 1\end{bmatrix}\end{bmatrix}\tau \tag{8}$$

where

$$(\theta_1, \theta_2, \dot{\theta}_1, \dot{\theta}_2) = (x_1, x_2, x_3, x_4) = x, \quad \tau = u. \tag{9}$$

Based on the constraint we wish to enforce in (2), choose

$$y = h(x) = 2x_1 + x_2 - \phi.$$

Then, following the procedure discussed above, we find that the Acrobot has relative degree 2 in terms of this "output," and (7) provides the input to maintain $y \equiv 0$, provided that initial conditions are chosen such that $y = \dot{y} = 0$. Furthermore, we note that in nonlinear control terminology, when the input in (7) is used in combination with the initial conditions $y = \dot{y} = 0$, then any resulting "internal" dynamics are referred to as the *zero dynamics* of the system [11]. Thus, (3) describes the zero dynamics of the Acrobot with respect to the output $2\theta_1 + \theta_2 - \phi$. An explicit expression for (7) for the Acrobot is easily derived (although somewhat tediously). The result is

$$\begin{aligned}\tau = (&-c_4(c_2 + c_3\cos\theta_2)\sin\theta_1 \\ &+ c_3(-(c_1 - c_2)\dot{\theta}_1^2 + 2c_2\dot{\theta}_1\dot{\theta}_2 + c_2\dot{\theta}_2^2 \\ &+ c_3\dot{\theta}_2^2\cos\theta_2)\sin\theta_2 + c_3^2\dot{\theta}_1\dot{\theta}_2\sin(2\theta_2) \\ &+ c_1 c_5\sin(\theta_1 + \theta_2) \\ &+ c_3 c_5\cos\theta_2\sin(\theta_1 + \theta_2))/(c_1 - c_2).\end{aligned} \tag{10}$$

As a final note, we mention that one can easily augment (7) [or (10) for the Acrobot] to produce exponential convergence to $y = 0$ if initial conditions do not satisfy $y = \dot{y} = 0$, but, again, this does not make an effective control approach for tracking a particular trajectory for the reasons mentioned earlier. In the next section we describe a suitable controller.

III. Tracking Controller

A. Control Law

In this section we present a control law for exactly tracking feasible trajectories of a nonlinear system. This control law is based on results for exponentially stable systems which are perturbed by a small, time-varying vector field [14] and has appeared elsewhere. Previously we used the nonlinear output tracking control law of Isidori and Byrnes [12], [11].[1] For the simple case of the Acrobot, the two approaches are equivalent.

[1]We are very grateful to Andy Teel for suggesting the Isidori-Byrnes nonlinear regulator and for providing additional assistance.

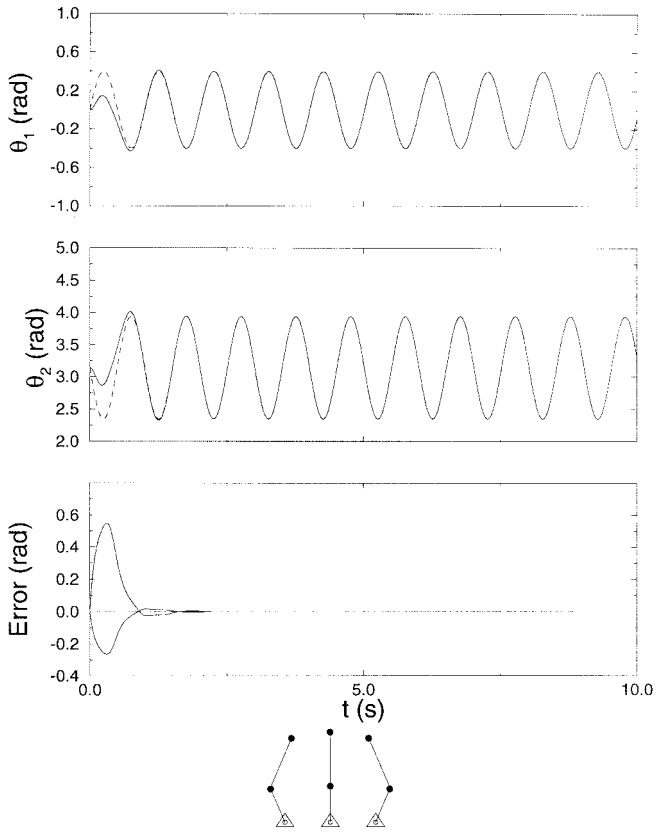

Fig. 4. Exact tracking using our controller.

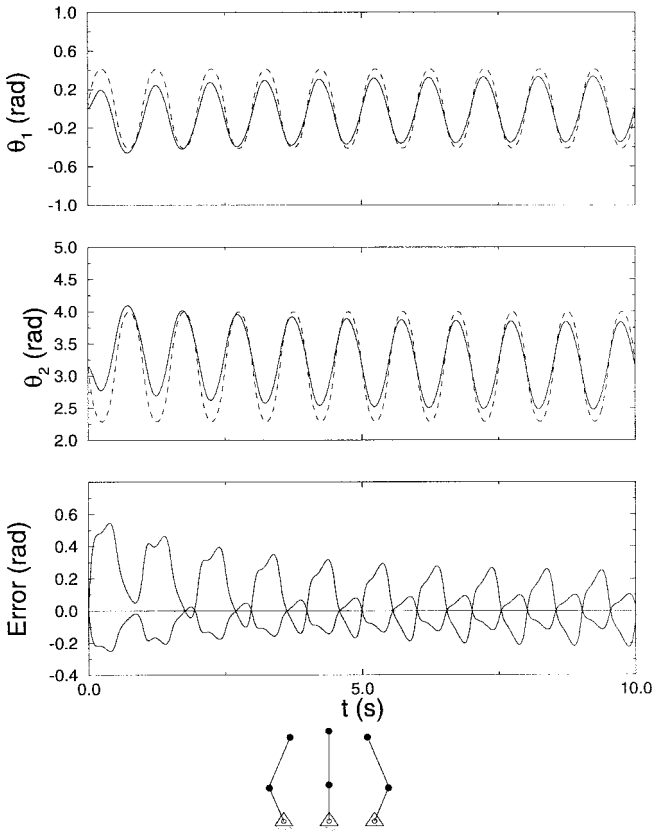

Fig. 5. Approximate tracking using pseudolinearization. The pseudolinearizing controller works well for slow trajectories (e.g., tracking a 0.1 Hz trajectory of the same amplitude produces small error), but for this 1 Hz trajectory, the performance is poor. Errors in θ_2 in the steady state reach ± 0.23 rad (13°).

Theorem 1: Consider the single input nonlinear system

$$\dot{x} = f(x) + g(x)u, \qquad x \in \mathbb{R}^n \tag{11}$$

where f and g are smooth n-dimensional vector fields. Suppose that $f(0) = 0$, and let $A = (\partial f/\partial x)(0)$, $b = g(0)$. Also, assume the pair (A, b) is completely controllable. We desire the state, $x(t)$, to exponentially track the trajectory $x_d(t) \in \mathbb{R}^n$, where $\|x_d(t)\| \leq c_1$ for all t with c_1 some positive constant. Suppose we have an input, $u = v(x_d(t))$, $v(0) = 0$, which produces the desired trajectory when the initial tracking error is zero. Thus

$$\dot{x}_d(t) = f(x_d(t)) + g(x_d(t))v(x_d(t)) \quad \text{for all } t. \tag{12}$$

Assume also that v is a smooth function of its argument. Let k be a row vector which makes $A + bk$ Hurwitz. Then, the input $u = v(x_d(t)) + k(x - x_d(t))$ produces local exponential tracking of the trajectory $x_d(t)$ if c_1 is sufficiently small.

Proof: Let $e = x - x_d(t)$ represent the tracking error. The closed loop dynamics in terms of e are then given by

$$\dot{e} = f(e + x_d(t)) + g(e + x_d(t))(v(x_d(t)) + ke) - \dot{x}_d(t). \tag{13}$$

Note that (12) shows that $e = 0$ is an equilibrium of this equation as expected. We must now show that $e = 0$ is also exponentially stable. First, write all functions as sums of constant, linear, and higher order terms

$$f(e + x_d(t)) = A(e + x_d(t)) + f_1(e + x_d(t))$$
$$g(e + x_d(t)) = b + \frac{\partial g}{\partial x}(0)(e + x_d(t)) + g_1(e + x_d(t))$$
$$v(x_d(t)) = \frac{\partial v}{\partial x}(0)x_d(t) + v_1(x_d(t))$$

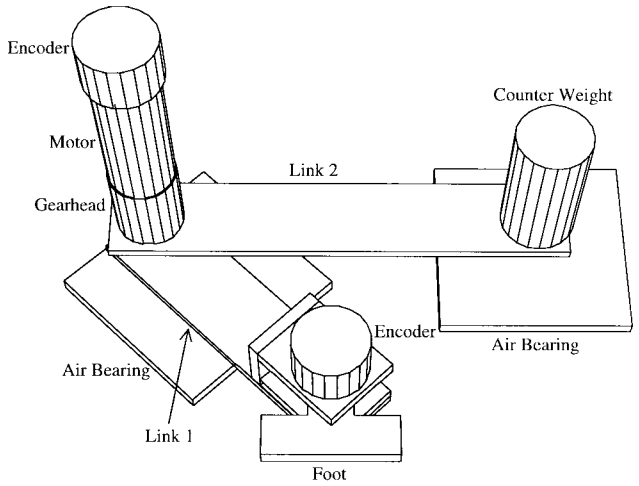

Fig. 6. Small acrobot. Link 1 is 10 cm long. Note that the first joint is unactuated. The gearhead on the motor was later removed.

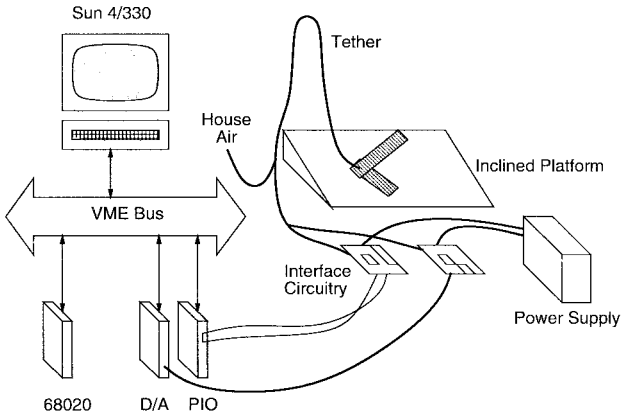

Fig. 7. Overall setup for Acrobot control experiments.

TABLE I
PARAMETER VALUES FOR THE SMALL ACROBOT

Param.	Value	Param.	Value
m_1	122 g	c_1	0.00433 kg-m^2
m_2	403 g	c_2	0.00506 kg-m^2
g	1.11 m/s^2	c_3	0.00338 kg-m^2
l_1	9.9 cm	c_4	0.0493 kg-m^2/s^2
l_{1cm}	3.8 cm	c_5	0.0379 kg-m^2/s^2
l_{2cm}	8.5 cm		
I_{1cm}	2,090 g-cm^2		
I_{2cm}	21,700 g-cm^2		

where $f_1(x)$ is defined to be $f(x) - Ax$, etc. Substituting these expressions into (13) gives

$$\dot{e} = A(e + x_d(t)) + b\left(\frac{\partial v}{\partial x}(0)x_d(t) + ke\right) + \beta(e, x_d(t)) - \dot{x}_d(t) \tag{14}$$

where $\beta(e, x_d(t))$ contains the nonlinear terms. Equation (14) must have the equilibrium $e = 0$, so

$$0 = Ax_d(t) + b\frac{\partial v}{\partial x}(0)x_d(t) + \beta(0, x_d(t)) - \dot{x}_d(t).$$

Substituting this into (14) gives

$$\dot{e} = (A + bk)e + [\beta(e, x_d(t)) - \beta(0, x_d(t))]. \tag{15}$$

We regard the second term on the right side of (15) as a perturbation to an exponentially stable system. It is given by [for simplicity we write x_d instead of $x_d(t)$]

$$\begin{aligned}\beta(e, x_d) - \beta(0, x_d) &= f_1(e + x_d) - f_1(x_d) \\ &\quad + \left(\frac{\partial g}{\partial x}(0)e + g_1(e + x_d) - g_1(x_d)\right) \\ &\quad \cdot \left(\frac{\partial v}{\partial x}(0)x_d + v_1(x_d)\right) \\ &\quad + \left(\frac{\partial g}{\partial x}(0)(e + x_d) + g_1(e + x_d)\right)ke\end{aligned}.$$

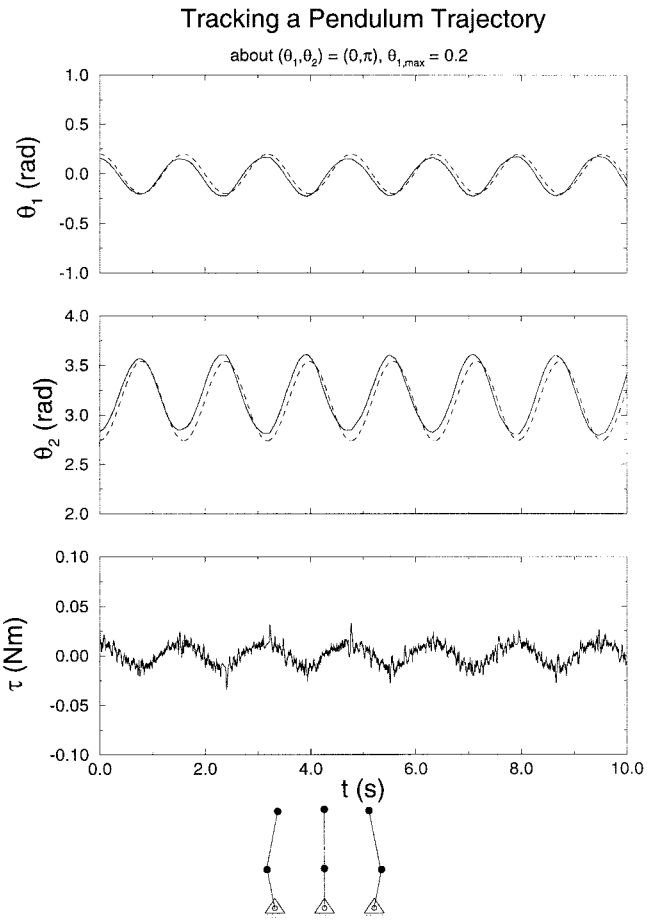

Fig. 8. Tracking experiment 1, $\phi = \pi$.

One can check that for any $\gamma > 0$, there exist constants c_1 and c_2 such that

$$\|\beta(e, x_d) - \beta(0, x_d)\| \le \gamma\|e\| \quad \text{for all } t \ge 0, \text{ for all } \|e\| < c_2$$

For example, consider the first 2 terms in the perturbation. By the mean value theorem we can write

$$\|f_1(e + x_d) - f_1(x_d)\| \le \left\|\frac{\partial f_1}{\partial x}(z)\right\|\|e\|$$

where z is a point on the line segment joining x_d to $x_d + e$. Recall that $(\partial f_1/\partial x)(0) = 0$. By continuity of $\partial f_1/\partial x$ we can make $(\partial f_1/\partial x)(z)$ as small as desired by making c_1 and c_2 sufficiently small.

As another example, consider the bound on the term

$$\left\|\frac{\partial g}{\partial x}(0)cke\right\| \le r\|e\|^2, \quad r = \left\|\frac{\partial g}{\partial x}(0)\right\|\|k\|.$$

For any $\gamma_3 > 0$ we need to be able to find a c_3 such that

$$r\|e\|^2 \le \gamma_3\|e\| \quad \text{for all } \|e\| < c_3.$$

This is easily done by choosing $c_3 = \gamma_3/r$.

That the remaining terms in the perturbation satisfy the requirement of being bounded by an arbitrarily small linear

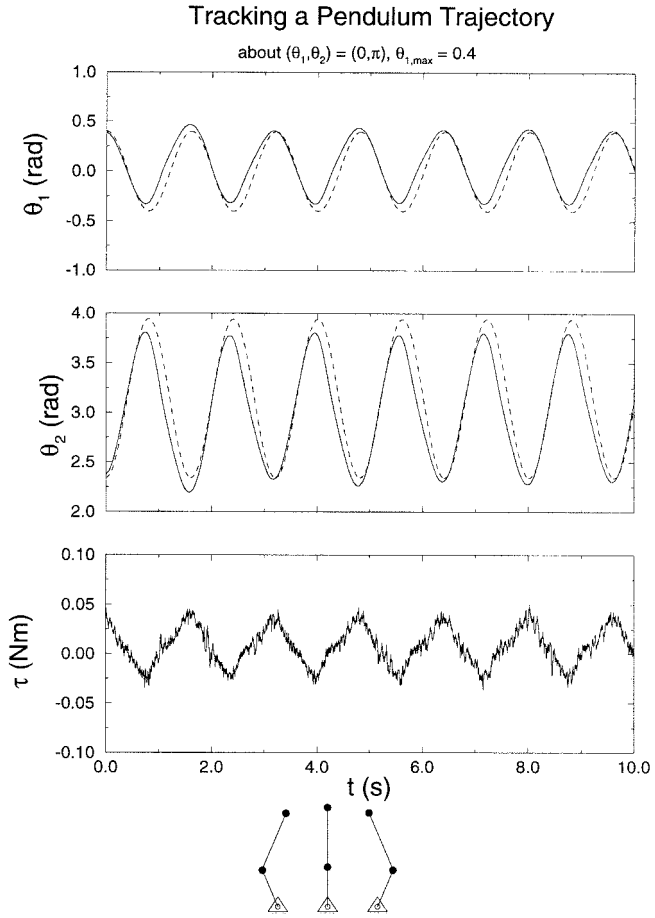

Fig. 9. Tracking experiment 2, $\phi = \pi$. The oscillation was about the same equilibrium as in Fig. 8, but this oscillation was twice as large. In fact, This was the largest magnitude oscillation that was achieved during experiments. Although there was significant error in the tracking, the performance was still fairly good. The peak-to-peak swing of θ_2 was about 85°.

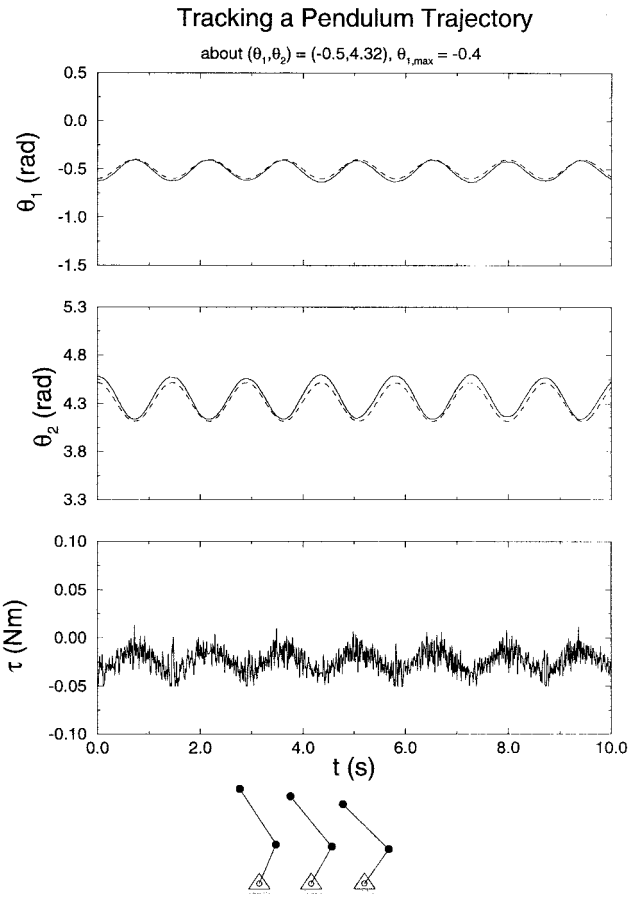

Fig. 10. Tracking experiment 3, $\phi = 3.32$.

growth in $\|e\|$ can easily be checked using similar methods. Thus, the origin $e = 0$ of the perturbed system (15) will be locally exponentially stable [14]. □

Remark: The proof in [14] involves use of the Lyapunov function for the unperturbed system on the perturbed system. In particular, choose $Q = Q^\top > 0$ and solve the Lyapunov equation

$$P(A+bk) + (A+bk)^\top P = -Q$$

for P. Then, $V(e) = e^\top Pe$ is a Lyapunov function for the unperturbed system, $\dot{e} = (A+bk)e$. Due to the properties of the perturbation term, $\beta(e, x_d(t)) - \beta(0, x_d(t))$, and under the stated assumptions, $V(e)$ can be shown to also be a Lyapunov function for the perturbed system.

B. Application to the Acrobot

To apply the controller to the Acrobot, we use the form of the equations of motion given by (8) and (9). Hauser and Murray [10] stated that the pair (A, b) was completely controllable for the Acrobot, which implies that poles can be placed arbitrarily using a linear feedback kx. We chose k to place all poles at -5 s^{-1}. $x_d(t)$ is chosen to be one of the pendulum trajectories discussed in Section II-B, and the input $v(x_d(t))$ is given by (10) with the state variables replaced by their desired values [(10) gives $v(x)$, while we want $v(x_d(t))$].

Strictly speaking, Theorem 1 only applies to the tracking of trajectories about the equilibrium

$$(\theta_1, \theta_2, \dot{\theta}_1, \dot{\theta}_2) = (0, 0, 0, 0)$$

since we assumed that $f(0) = 0$, $v(0) = 0$, etc. Application to other equilibria is easily accomplished through coordinate transformations and by redefining functions. In particular, suppose we are interested in the equilibrium configuration (x^o, u^o), where

$$0 = f(x^o) + g(x^o)u^o.$$

Then, redefining the system (x, u, f, g) according to

$$\hat{x} = x - x^o, \quad \hat{u} = u - u^o$$
$$\hat{f}(\hat{x}) = f(\hat{x} + x^o) + g(\hat{x} + x^o)u^o, \hat{g}(\hat{x}) = g(\hat{x} + x^o)$$

gives a new system $(\hat{x}, \hat{u}, \hat{f}, \hat{g})$ which satisfies the assumptions and has the dynamics of the original system about the original equilibrium. Also, we can define

$$\hat{x}_d(t) = x_d(t) - x^o, \quad \hat{v}(\hat{x}_d(t)) = v(\hat{x}_d(t) + x^o) - u^o.$$

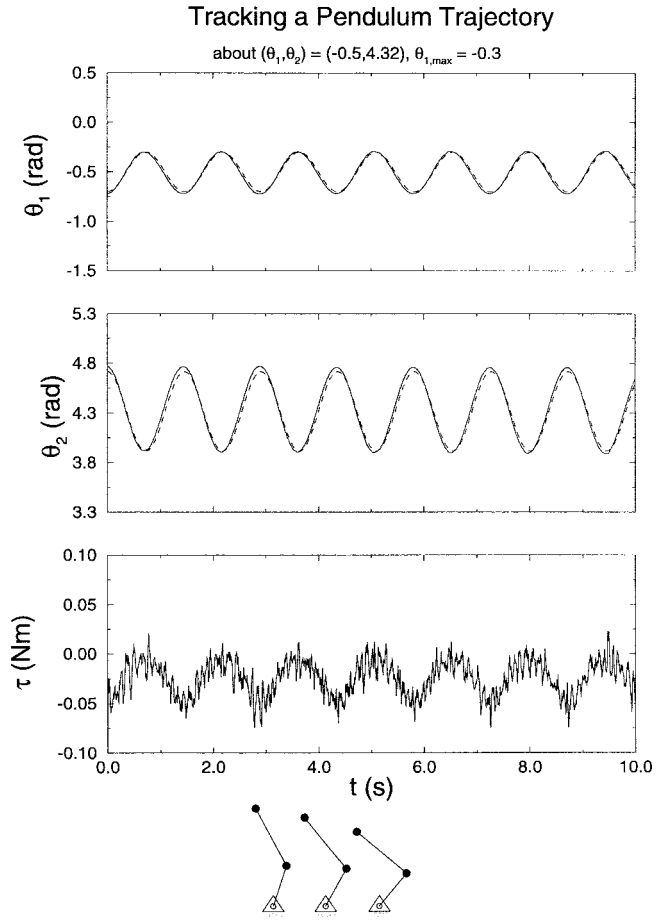

Fig. 11. Tracking experiment 4, $\phi = 3.32$. The oscillation was about the same equilibrium configuration as in Fig. 10. These results showed the least error of all the tracking experiments. Note that the torque periodically exceeded the maximum continuous torque the motor could provide (0.03 Nm in magnitude). The motor became excessively warm after running this experiment for a period of time.

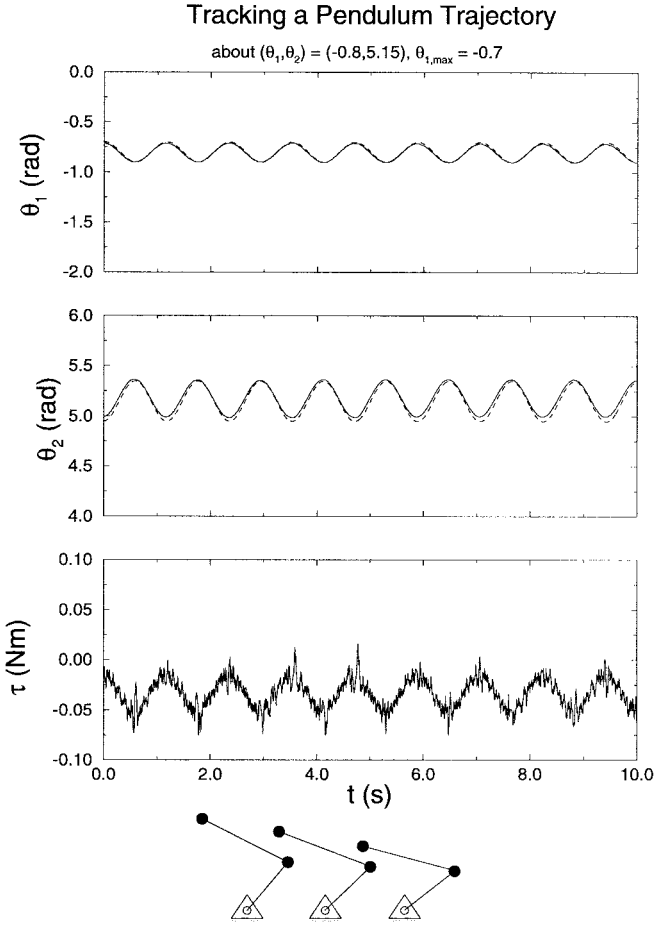

Fig. 12. Tracking experiment 5, $\phi = 3.55$. Note again that the torque required periodically exceeded the maximum continuous torque the motor could provide.

IV. Simulations

Hauser and Murray [10] and Bortoff and Spong [9] applied linearization methods to track inverted trajectories of the Acrobot. In this section we offer simulation results to compare our controller with a specific linearization method called pseudolinearization. This is exactly the method used by Bortoff and Spong, and Murray and Hauser also compared pseudolinearization to their method in [17]. Results for the two were very similar.

Pseudolinearization was introduced by Reboulet and Champetier [20], although we have used the equivalent (but simpler) approach of Wang and Rugh [27]. Pseudolinearization can be applied to a system with a continuum of equilibria. It is a gain scheduling method, in that the linear approximation to the system about the equilibrium "closest" to the current state is used to compute feedback gains. Because the feedback is based on a linear approximation to the system, trajectories to be tracked must always remain near the set of equilibria. We briefly present a restricted summary of the pseudolinearization method here, based on [27].

Consider the single input nonlinear system in (11). Assume there is a family of "operating points" $\{(\boldsymbol{x}(\alpha), \boldsymbol{u}(\alpha)), \alpha \in \Gamma\}$, $\Gamma \subset \mathbb{R}$, satisfying $f(\boldsymbol{x}(\alpha)) + g(\boldsymbol{x}(\alpha))\boldsymbol{u}(\alpha) = 0$ for all $\alpha \in \Gamma$ (The Acrobot is such a system with $\alpha = \phi$, θ_1, or θ_2, for example). Assume that the linear approximation to the nonlinear system (11) is completely controllable about all operating points. In the pseudolinearization method one seeks an invertible state variable change, $z = P(x)$, $z \in \mathbb{R}^n$ and feedback law, $u = P_{n+1}(x, w)$, $w \in \mathbb{R}$, such that when the new system with state z and input w is linearized about its family of operating points, $\{(\boldsymbol{z}(\alpha), \boldsymbol{w}(\alpha)), \alpha \in \Gamma\}$, the result is a constant system consisting of a chain of integrators

$$\frac{d}{dt}(z - \boldsymbol{z}(\alpha)) = \begin{bmatrix} 0 & 1 & \cdots & 0 & 0 \\ \vdots & \vdots & & \vdots & \vdots \\ 0 & 0 & \cdots & 0 & 1 \\ 0 & 0 & \cdots & 0 & 0 \end{bmatrix} (z - \boldsymbol{z}(\alpha)) + \begin{bmatrix} 0 \\ \vdots \\ 0 \\ 1 \end{bmatrix} (w - \boldsymbol{w}(\alpha)).$$

It is also shown in [27] that $\boldsymbol{w}(\alpha) = 0$, and $\boldsymbol{z}_i(\alpha) = 0$, $i = 2, 3, \cdots, n$. Once this has been accomplished, a feedback law can easily be derived for the integrator chain to achieve some goal (such as stabilization or tracking) in the z state space. [27] contains explicit representations for the mappings $z = P(x)$,

$u = P_{n+1}(x, w)$, but they are sufficiently complicated that we won't repeat them here.

In our implementation, $n = 4$, and we used $\alpha = \theta_1$. Thus, at a given time, the value of the Acrobot's first joint angle determined the linear approximation that was used in computing linear feedback gains on errors. z_4 was made to track a 1 Hz sinusoid by appropriate choice of input w and feedback gains on the error. The magnitude of the sinusoid was chosen to produce oscillations in $x(t) = P^{-1}(z(t))$ comparable to those used for our control law. Unfortunately, it was not possible to use the pseudolinearizing controller to track the identical pendulum trajectories that were tracked by our controller (this would provide a better comparison). The obvious reason for this is that feasible $x(t)$ trajectories (i.e., state trajectories for the Acrobot for which there exist an input to produce them) do not correspond to feasible $z(t)$ trajectories ($z(t)$ must satisfy the chain of integrators equation, which is only an approximation to the actual nonlinear dynamics).

Figs. 4 and 5 show simulation results for the two different nonlinear controllers. Solid lines are the actual trajectories, while dashed lines show the desired trajectories. Acrobot parameter values were those given earlier in Section II. Gains for both controllers were chosen to place all poles at -5 s^{-1}. Initial conditions were $(\theta_1, \theta_2, \dot{\theta}_1, \dot{\theta}_2) = (0, \pi, 0, 0)$ for both simulations. The stick figures show extreme and midpoint configurations of the desired motion, as described in Fig. 2. Not surprisingly, pseudolinearization produces unsatisfactory results at this frequency, with a tracking error of $\pm 13°$ for θ_2.

For tracking fast periodic inverted trajectories, our controller clearly does much better than the pseudolinearizing controller. However, we are limited to the specific pendulum oscillations that were derived in Section II-B. In order to modify the frequency of oscillation, physical parameters of the Acrobot would need to be changed. The set of trajectories is reasonably rich, though, in that the amplitude and the point about which the oscillations occur are free parameters. The pseudolinearization approach is somewhat more general in that one is free to choose $z_4(t)$ to be any desired function of time. However, the selected trajectory much keep the Acrobot close to its set of inverted equilibrium positions, or the performance will be poor.

V. Experiments

Our controller is guaranteed to work for a trajectory with sufficiently small amplitude and for an initial tracking error which is sufficiently small. Of course, the proof of the result also assumes exact parameter values are available, etc. We wished to determine the performance of the controller on a physical system with unmodeled characteristics such as joint friction, inexact parameter values, tether disturbances, etc. As shall be seen, we found that large amplitude oscillations could be tracked without much difficulty, even in the presence of these real-world effects.

A. Hardware Description

A Small Acrobot: We constructed a small Acrobot which was designed to operate on a slightly tilted plane in order to scale gravity. This allowed a relatively small motor to be used as the actuator at the second joint and also inexpensive plastic parts to be used in the construction. A 20 W rare earth DC motor from Maxon (model #RE025-055-37EBA201AB) was used to provide the actuation. Originally, it was coupled to a $4.33:1$ planetary gearhead also from Maxon. It was thought that a low ratio gearhead would provide amplification of the torque without significant friction or backlash. Unfortunately, although the backlash was small, it was enough to prevent control for trajectories where the gears unmeshed. For this reason the gearhead was later removed, and performance increased substantially. A passive foot was attached to the first link since one of our motivations was to study locomotion issues with the Acrobot. Optical encoders were used for position sensing.

The robot had air bearings to levitate it off a smooth piece of glass. Air hose was routed back to a house supply through the robot's tether. A platform with adjustable tilt angle (set at $6.5°$ in experiments) held the glass. A compromise was necessary in the choice of the angle for the tilting platform since too great an angle meant excessive actuator forces were necessary to overcome gravity, while too shallow an angle meant that the forces of the robot's tether were a significant disturbance to the dynamics. Fig. 6 shows the components of the small Acrobot.

1) Computer Control: A 68 020-based single board computer in a VME card cage was used to execute the control software. Software written at UC Berkeley[2] made it possible to program in C and to easily communicate with the cards in the VME cage. The control software was written and compiled on a Sun 4/330 workstation and then downloaded to the single board computer. The control loop was run at 500 Hz. A digital implementation of a differentiator in series with a second-order Butterworth filter was used to provide an approximation to the joint velocities. The cut-off frequency of the filter was set to 10 Hz.

2) Interface Circuitry: The circuitry consisted of both analog and digital components. A voltage-controlled current source was built using two National Semiconductor LM12 op-amps and miscellaneous discrete components. One output on the D/A board was connected to the voltage input of the circuit, and the current output drove the motor. Since the torque of a DC motor is linearly related to the current through its rotor windings, this circuit provided a means for the computer to specify the torque at the second joint. Two HP HCTL-2020 quadrature decoder/counter chips were used to read and store the encoder outputs. The outputs from the chips were connected to a Parallel I/O board in the VME Card Cage. Fig. 7 shows the overall setup.

B. Parameter Determination

Simulations showed the importance of accurately determining the parameters. The robot was disassembled and all the individual parts were independently weighed and measured. This produced sufficiently accurate parameter values for good performance. Table I shows the parameter values used in the control law. Another approach would be to use an online

[2] Authored by R. Murray.

parameter estimation scheme. Spong and Block [25] reported good results for their pendubot using this type of method.

Simulations showed that the absolute values of the joint angles needed to be known within 2° or so. To achieve this, the robot was hung upside down on the inclined plane and left alone until it came to rest. This gave the encoder values for the $(\theta_1, \theta_2) = (0, \pi)$ configuration (straight up).

C. Results

Tracking experiments were performed for pendulum oscillations about three different equilibrium configurations. The foot was fixed firmly in place at all times. Table I parameter values were used for all experiments. The row vector k, however, was different for each equilibrium configuration (or value of ϕ). This was because k was chosen to place the poles of $A + bk$ at -5 s^{-1}, and A was a function of the equilibrium configuration. A major problem encountered in experiments was the influence of the tether on the behavior of the robot. The tether was attached to the robot from the ceiling and would pull on the robot when displaced from its equilibrium position. Care was taken to try to position the robot at the neutral position of the tether at the beginning of each experiment. Another problem was overheating of the motor for equilibrium configurations other than straight up. At these configurations a nominal "holding torque" was required to maintain θ_2 in equilibrium. The further the equilibrium configuration was from $(\theta_1, \theta_2) = (0, \pi)$, the larger was the necessary torque. This meant that for these configurations, the experiments had to be done quickly to avoid damaging the motor.

Figs. 8–12 show the tracking experiment results. Solid lines are the actual trajectories, while dashed lines show the desired trajectories. All plots of θ_1 are scaled the same for easy comparison of amplitudes. The same is true for θ_2 and τ. Also included are stick figures of the Acrobot's motion, which should be interpreted as in Fig. 2. Figs. 8 and 9 show two different magnitudes of oscillation about the $(0, \pi)$ configuration. Fig. 9 is the largest magnitude oscillation that was obtained in all the experiments. Notice that the peak-to-peak swing of θ_2 is around 85°. Figs. 10 and 11 show two different magnitudes of oscillation about the $(-0.5, 4.32)$ configuration. Fig. 12 shows an oscillation about the $(-0.8, 5.15)$ configuration. The torque plotted in the figures is the commanded torque, not the actual applied torque (although the two are assumed to be fairly similar). The noise in the commanded torque was probably due to the feedback's dependence on the joint velocities, which were estimated from encoder readings (as described earlier).

In addition to the tether, possible sources of error were small amounts of friction in joint 1, differences between commanded torque and applied torque, inexact parameter values, and noisy and delayed joint velocity data.

VI. Conclusion

In this paper we have presented a new approach to the Acrobot control problem. Rather than relying on a linear approximation of the Acrobot near the set of equilibrium configurations as in [4], [9], [10], [19], we have found a surprising set of exact trajectories of the nonlinear equations. These trajectories involved periodic inverted motions of the Acrobot and were shown to be noninverted pendulum oscillations. The trajectories also had the interpretation of the zero dynamics of the output $2\theta_1 + \theta_2 - \phi$. We presented a nonlinear control law (which has appeared elsewhere) and showed how it could be applied to the Acrobot to track these trajectories. We believe our work nicely illustrates the use and utility of this tracking controller. We described a physical implementation of the Acrobot and experimental results which demonstrated that the assumptions of the theory were not overly restrictive. In particular, peak-to-peak oscillations of θ_2 as large as 85° were obtained, despite real-world effects, such as joint friction, inexact parameter values, and noisy and delayed joint velocity data. Available motor torque was a limiting factor in experiments. Our work should suggest new approaches for the general underactuated manipulator problem. In addition, our work has applications to legged robot locomotion [7].

Good tracking results for [9], [10] were obtained when using frequencies around 0.1 Hz. Our approach allows for the tracking of much higher frequency oscillations by making appropriate choices of mass and length parameters. In particular, we compared simulations of a pseudolinearizing controller and our controller at 1 Hz. Our controller produced no error, while the pseudolinearizing controller had an error of ± 0.23 rad (13°) in θ_2. In our experiments we tracked 0.63 Hz trajectories.

Acknowledgment

The authors would like to thank A. Teel and R. Murray as cited earlier, P.-H. Arnaud and Y. Matsuoka for assistance in constructing experimental hardware, Ph.D. committee members S. S. Sastry and R. Littlejohn for their comments, and the anonymous reviewers for their help.

References

[1] H. Arai and S. Tachi, "Position control of a manipulator with passive joints using dynamic coupling," *IEEE Trans. Robot. Automat.*, vol. 7, pp. 528–534, Aug. 1991.

[2] H. Arai, K. Tanie, and S. Tachi, "Dynamic control of a manipulator with passive joints in operational space," *IEEE Trans. Robot. Automat.*, vol. 9, pp. 85–93, Feb. 1993.

[3] J. Baillieul, "The behavior of single-input super-articulated mechanisms," in *Proc. 1991 Amer. Contr. Conf.*, 1991, pp. 1622–1626.

[4] N. S. Bedrossian, "Nonlinear control of an underactuated two-link manipulator," in *Proc. 1993 Amer. Contr. Conf.*, 1993, pp. 2234–2238.

[5] M. Bergerman, C. Lee, and Y. Xu, "A dynamic coupling index for underactuated manipulators," *J. Robot. Syst.*, vol, 12, no. 10, pp. 693–707, Oct. 1995.

[6] M. Bergerman and Y. Xu, "Optimal control sequence for underactuated manipulators," in *Proc. 1996 IEEE Int. Conf. Robot. Automat.*, 1996, pp. 3714–3719.

[7] M. D. Berkemeier and R. S. Fearing, "Sliding and hopping gaits for the underactuated acrobot," *IEEE Trans. Robot. Automat.*, vol. 14, pp. 629–634, Aug. 1998.

[8] S. A. Bortoff, *Pseudolinearization Using Spline Functions with Application to the Acrobot*, Ph.D. dissertation, Univ. Illinois, Urbana-Champaign, 1992.

[9] S. A. Bortoff and M. W. Spong, "Pseudolinearization of the acrobot using spline functions," in *Proc. 31st IEEE Conf. Decision Contr.*, 1992, pp. 593–598.

[10] J. Hauser and R. M. Murray, "Nonlinear controllers for nonintegrable systems: The Acrobot example," in *Proc. 1990 Amer. Contr. Conf.*, 1990, pp. 669–671.

[11] A. Isidori, *Nonlinear Control Systems*, 3rd ed. New York: Springer-Verlag, 1995.
[12] A. Isidori and C. I. Byrnes, "Output regulation of nonlinear systems," *IEEE Trans. Automat. Contr.*, vol. 35, pp. 131–140, Feb. 1990.
[13] A. Jain and G. Rodriguez, "An analysis of the kinematics and dynamics of underactuated manipulators," *IEEE Trans. Robot. Automat.*, vol. 9, pp. 411–422, Aug. 1993.
[14] H. K. Khalil, *Nonlinear Systems*, 2nd ed. Englewood Cliffs, NJ: Prentice-Hall, 1996.
[15] I. Kolmanovsky and N. H. McClamroch, "Developments in nonholonomic control problems," *IEEE Contr. Syst. Mag.*, vol. 15, pp. 20–36, Dec. 1995.
[16] M. A. Lee and M. H. Smith, "Automatic design and tuning of a fuzzy system for controlling the Acrobot using genetic algorithms, DSFS, and meta-rule techniques," in *Proc. 1st Int. Joint Conf. North Amer. Fuzzy Inform. Process. Soc. Biannu. Conf.*, 1994, pp. 416–420.
[17] R. M. Murray and J. Hauser, "A case study in approximate linearization: The acrobot example," Tech. Rep. UCB/ERL M91/46, Univ. California, Berkeley, 1991.
[18] G. Oriolo and Y. Nakamura, "Control of mechanical systems with second-order nonholonomic constraints: Underactuated manipulators," in *Proc. 30th IEEE Conf. Decision Contr.*, 1991, pp. 2398–2403.
[19] S. Pannu, H. Kazerooni, G. Becker, and A. Packard, "μ-synthesis control for a walking robot," *IEEE Contr. Syst. Mag.*, vol. 16, pp. 20–25, Feb. 1996.
[20] C. Reboulet and C. Champetier, "A new method for linearizing nonlinear systems: The pseudolinearization," *Int. J. Contr.*, vol. 40, no. 4, pp. 631–638, 1984.
[21] M. Reyhanoglu, A. van der Schaft, and N. H. McClamroch, "Dynamics and control of second-order nonholonomic systems," in *Proc. 35th IEEE Conf. Decision Contr.*, 1996.
[22] F. Saito, T. Fukuda, and F. Arai, "Swing and locomotion control for a two-link brachiation robot," *IEEE Contr. Syst. Mag.*, vol. 14, pp. 5–12, Feb. 1994.
[23] D. Seto and J. Baillieul, "Control problems in super-articulated mechanical systems," *IEEE Trans. Automat. Contr.*, vol. 39, pp. 2442–2253, Dec. 1994.
[24] M. W. Spong, "The swing up control problem for the Acrobot," *IEEE Contr. Syst. Mag.*, vol. 15, no. 1, pp. 49–55, 1995.
[25] M. W. Spong and D. J. Block, "The pendubot: A mechatronic system for control research and education," in *Proc. 34th IEEE Conf. Decision Contr.*, 1995, pp. 555–556.
[26] M. W. Spong and M. Vidyasagar, *Robot Dynamics and Control*. New York: Wiley, 1989.
[27] J. Wang and W. J. Rugh, "On the pseudo-linearization problem for nonlinear systems," *Syst. Contr. Lett.*, vol. 12, pp. 161–167, 1989.

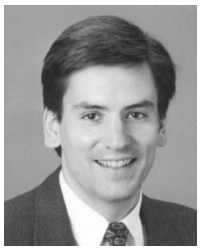

Matthew D. Berkemeier received the B.S. degree in electrical engineering from Purdue University, West Lafayette, IN, in 1987 and the M.S. and Ph.D. degrees in electrical engineering from the University of California at Berkeley, in 1990 and 1993, respectively.

From 1993 to 1998, he was an Assistant Professor in the Aerospace and Mechanical Engineering Department, Boston University, Boston, MA. He joined the Electrical and Computer Engineering Department, Utah State University, Logan, in 1999. His research interests include mobile robot locomotion and the control of underactuated robots.

Dr. Berkemeier received the NSF CAREER award in 1998.

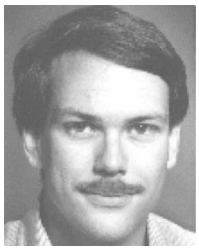

Ronald S. Fearing received the S.B. and S.M. degrees in electrical engineering and computer science from the Massachusetts Institute of Technology, Cambridge, in 1983 and the Ph.D. degree in electrical engineering from Stanford University, Stanford, CA, in 1988.

He is an Associate Professor in the Department of Electrical Engineering and Computer Sciences, University of California, Berkeley, which he joined in 1988. His principle research interests are in tactile sensing, teletaction, microrobotics, and dextrous manipulation.

Dr. Fearing received the Presidential Young Investigator Award in 1991.